File Revision Date :

December 8, 2025

Data Set Description:

PI:	Michaël Sicard
Instrument:	Elastic, backscatter lidar "LiO3S"
Site:	OPAR-StPaulMaido, Reunion island (21° S, 55° E, 2158 m a.s.l.)
Measurement Quantities:	Vertical profiles of particle backscatter coefficient at 355 nm (10-45 km)

Contact Information:

Name:	Michaël Sicard
Institute:	LACy, UMR 8105 UR CNRS MF, Université de la Réunion
Adresse :	15, avenue René Cassin – CS 92003, 97744 Saint-Denis, France Cédex 9
Phone:	+262 2 62 52 89 63
Email:	michael.sicard@univ-reunion.fr

Instrument Description:

(See Figures 1 and 2) The emission set-up consists in two different lasers. A XeCl PulseMaster PM-800 Series excimer laser, from LightMachinery, emits electromagnetic pulses at 308 nm wavelength with a frequency of 40 Hz and pulse energy of 220 mJ. A Nd: YAG Lab 150 laser from Spectra-Physics emits electromagnetic pulse at a 1064 nm wavelength with a frequency of 30 Hz. The final wavelength emitted by the Nd: YAG laser is 355 nm, corresponding to the third harmonic of the emitted wavelength. The pulse energy at this wavelength is 130 mJ. The laser beam diameter is about 10 mm, and its divergence is 0.5 mrad. The optical design of this lidar is represented in Figure 2. Again, the emission and reception of this lidar are located in different rooms, explaining the use of many mirrors. The expander consists in three lenses, BE1, BE2 and BE3, magnifying the signal by a factor 10. The final beam has a 100 mm diameter.
The reception is made of four 500 mm diameter telescopes. The primary mirrors are M1, M2, M3 and M4. The signal is emitted at the center of these telescopes, and the distance between the emission and the center of each telescope is 600 mm. At the receiving end, the signal is a focused from each telescope to a corresponding optical fiber, which are positioned in line before entering the detection box. In this box, a diffraction grating separates the different wavelengths. Internal mirrors allow the beam to be reflected in the detectors. Finally, a glass plate discriminates the high and low energy channels at 355 nm.
All the detectors are PMT from Hamamatsu and the signal acquisition cards are from Licel. The 355 nm detectors are electronically shuttered to avoid saturation. The acquisition is in photocounting mode only for the high energy channels, and in photocounting and analog mode for the low energy channels. Raw files follow a 1minute integration.

Algorithm Description:

Data processing levels range from Level 0 to Level 2.

- Level 0 products (L0) are uncorrected and uncalibrated raw data files in Licel format at full resolution produced by the instrument.
- Level 1 products (L1) provide cloud-free data cleaned from any instrumental artifact (electronic parasites, synchronization problems, power disrupt, etc.). The cloud mask is

currently manual. These corrections are essential for any user to be able to apply their own specific aerosol preprocessing without errors linked to the instrument itself or the weather.

- Level 2 products (L2) provide processed lidar data including: saturation correction, background-sky correction, geometrical form factor correction and gluing between high and low-energy channels (L2a). These products also provide the aerosol optical properties and their corresponding uncertainties (L2b).

Only L2b data are publicly available. Most important is the inversion method used. This dataset has been inverted with the two-component Klett inversion (Klett, 1981; 1985) assuming a constant lidar ratio of 50 sr. More details on Level 1 and 2 production can be found in Gantois et al. (2024).

Expected Precision/Accuracy of Instrument:

The total uncertainty budget is described in Appendix B of Gantois et al. (2024) and summarized in Table 1. Four sources of uncertainty were propagated in quadrature (Sicard et al., 2009; Rocadenbosch et al., 2010): (i) uncertainty due to the Rayleigh calibration value, (ii) uncertainty due to the lidar ratio value with a distinction between LR, top and LR, bottom defining the respective upper and lower error bars, (iii) uncertainty due to the SNR vertical distribution, (iv) and uncertainty due to the SNR value at the calibration altitude.

The uncertainty analyses reveal a strong influence of the LR value in the low-altitude ranges and a strong influence of the SNR in the high-altitude ranges. Uncertainty values relative to the total backscatter coefficient are low. Uncertainty values relative to the aerosol backscatter coefficient are high because of the very low aerosol backscatter coefficient values generally observed above Maïdo observatory.

Instrument history and perspectives:

The OPAR LiO3S lidar delivers aerosol optical products (backscatter coefficients at 355 nm) since May 2013. The preprocessed (L1), processed (L2a) and inverted (L2b) data have been performed in an automated and harmonized manner. Uncertainties have been estimated following state-of-the-art formulations of lidar uncertainty budget. The lidar is operated two nights/week on Monday and Tuesday night from approximately 19 to 01:00 LT. During EarthCARE overpasses, measurements are extended until at least 04:00 LT. OPAR-StPaulMaido aerosol lidars are participating to EarthCARE cal/val exercise in the framework of ESA EVID 05 (ACTRIS-EU) and EVID 15 (ACTRIS-FR) projects. Data of this instruments have been used recently in Baron et al. (2023) and Sicard et al. (2025).

A new lidar called TAMARIN (Temperature Aerosol huMidity lidAr at Reunion IslaNd) is currently under development within the CNRS-INSU funded GON lidar project (2022-2025), aiming at a major upgrade and automation of the OHP and OPAR lidar parks. TAMARIN is designed to measure unmanned, unattended 7 nights/week the profiles of water vapor and aerosols. Elastic parallel, elastic perpendicular and Raman channels are planned at both 355 and 532 nm. TAMARIN should be included in the ACTRIS European research infrastructure and, as such, all optical products will be delivered by the Single Calculus Chain of ACTRIS. When all aerosol products of TAMARIN are validated, only TAMARIN aerosol products will be sent to both ACTRIS and NDACC database.

Reference Articles:

Baron, A., Chazette, P., Khaykin, S., Payen, G., Marquestaut, N., Bègue, N., and Duflot, V.: Early Evolution of the Stratospheric Aerosol Plume Following the 2022 Hunga Tonga-Hunga Ha'apai

Eruption: Lidar Observations From Reunion (21°S, 55°E), Geophys. Res. Lett., 50, e2022GL101751, https://doi.org/10.1029/2022GL101751, 2023.

Gantois, D., Payen, G., Sicard, M., Duflot, V., Bègue, N., Marquestaut, N., Portafaix, T., Godin-Beekmann, S., Hernandez, P., and Golubic, E.: Multiwavelength aerosol lidars at the Maïdo supersite, Réunion Island, France: instrument description, data processing chain, and quality assessment, Earth Syst. Sci. Data, 16, 4137–4159, https://doi.org/10.5194/essd-16-4137-2024, 2024.

Klett, J. D.: Stable analytical inversion solution for processing lidar returns, Appl. Opt., 20, 211, https://doi.org/10.1364/AO.20.000211, 1981.

Klett, J. D.: Lidar inversion with variable backscatter/extinction ratios, Appl. Opt., 24, 1638, https://doi.org/10.1364/AO.24.001638, 1985.

Rocadenbosch, F., Md. Reba, M. N., Sicard, M., and Comerón, A.: Practical analytical backscatter error bars for elastic one-component lidar inversion algorithm, Appl. Opt., 49, 3380, https://doi.org/10.1364/AO.49.003380, 2010.

Sicard, M., Comerón, A., Rocadenbosch, F., Rodríguez, A., and Muñoz, C.: Quasi-analytical determination of noise-induced error limits in lidar retrieval of aerosol backscatter coefficient by the elastic, two-component algorithm, Appl. Opt., 48, 176, https://doi.org/10.1364/AO.48.000176, 2009.

Sicard, M., Baron, A., Ranaivombola, M., Gantois, D., Millet, T., Sellitto, P., Bègue, N., Bencherif, H., Payen, G., Marquestaut, N., and Duflot, V.: Radiative impact of the Hunga stratospheric volcanic plume: role of aerosols and water vapor over Réunion Island (21° S, 55° E), Atmos. Chem. Phys., 25, 367–381, https://doi.org/10.5194/acp-25-367-2025, 2025.

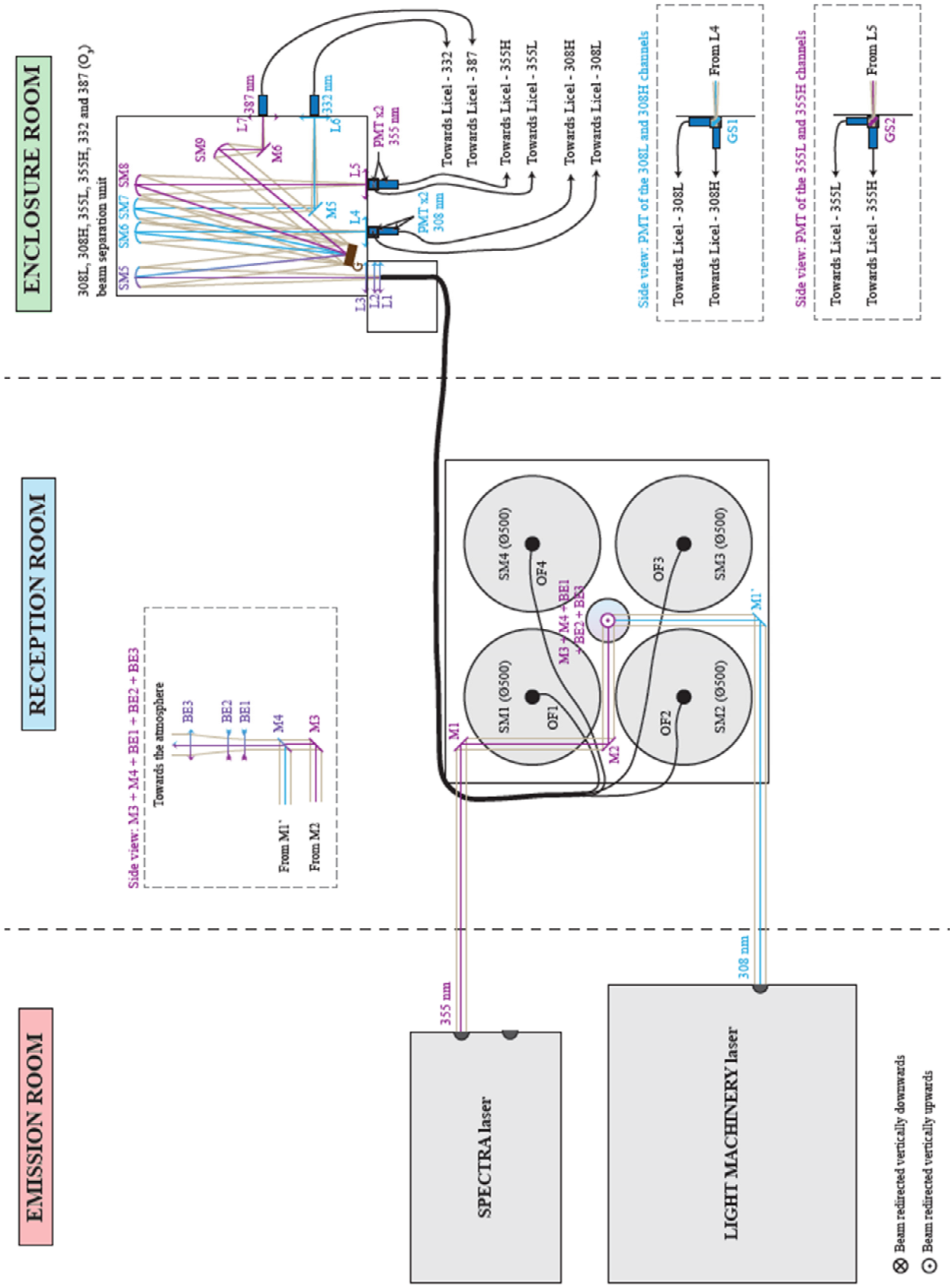

Figure 1: LiO3S optical scheme.

LIO3S	ID OPTICAL SCHEME	TYPE
EMISSION	M1, M3	Rmax 355 nm (Ø= 40 ou 50 mm)
	M2	Rmax 355 nm (Ø= 1'')
	M4	Dichroic mirror T355 nm, R308 nm (Ø= 50.8 mm)
	BE1, BE2	Achromat lenses (f= -500 mm)
	BE3	Lens (f= +1500 mm)
	M1'	Rmax 308 nm (Ø= 50 mm)
RECEPTION	SM1, …, SM4	Primary mirrors (Ø= 0.5 m, f= +1.5 m)
	OF1, …, OF4	Optical fibers (Ø= 1 mm)
308L, 308H, 355L, 355H, 332 AND 387 BEAM SEPARATION UNIT (O_3)	L1, L2	Lens (f= +20 mm)
	L3	Lens (f= +75 mm)
	SM5, …, SM9	Spherical mirror (f= +600 mm)
	G	Grating 3600 slits/mm
	L4, …, L7	Lens (f= +30 mm)
	GS1, GS2	Glass slide 96/4
	M5, M6	Folding mirror
	308L PMT	?
	308H PMT	?
	332 PMT	?
	355L PMT	R7400P-03G (HB9287)
	355H PMT	R7400P-03G (HC2163)
	387 PMT	P03 (HB3622)

Figure 2: Specifications of LiO3S optics.

Uncertainty source	Equation
Uncertainty due to the Rayleigh calibration value (u_{altref})	$$u_{altref} = \left\lvert \left(\frac{\beta_j}{\beta_N}\right)^2 \frac{U_N}{U_j} \right\rvert \sigma_{\beta_N}$$
Uncertainty due to the lidar ratio value (u_{LR})	$$u_{LR} = \left\lvert \pm p \frac{2\beta_j^2}{U_j} G_j + p^2 \frac{4\beta_j^3}{U_j^2} {G_j}^2 \right\rvert$$ Where: $G_j = \sum_{i=j}^{N} w_i S_i U_i$
Uncertainty due to the SNR vertical distribution (u_{SNR}).	$$u_{SNR} = \sqrt{\left(\frac{\beta_j}{U_j}\right)^2 \sigma_{U_j}^2 + \left(\frac{2\beta_j}{U_j}\right)^2 \sigma_{GU_j}^2}$$ Where: $\sigma_{GU_j}^2 = \sum_{k=j}^{N} (w_k S_k)^2 {\sigma_{U_k}}^2$
Uncertainty due to the SNR value at the calibration altitude ($u_{SNR,altref}$).	$$u_{SNR,altref} \approx \left\lvert \frac{\beta_j^2}{\beta_N U_j} \right\rvert \sigma_{U_N}$$

Table 1: Total-Backscatter analytical error bars from Klett's backward inversion method (from Rocadenbosch et al., 2010).